Journal **XX** (XXXX) XXXXXX https://doi.org/XXXX/XXXX

Enhanced Helium Exhaust During Edge-Localized Mode Suppression by Resonant Magnetic Perturbations at DIII-D

E. T. Hinson,[1*] O. Schmitz,[1] T. Abrams,[2] A. Briesemeister,[3] I. Bykov,[5] C. Chrystal,[2] C. Collins,[2] T. E. Evans,[2] H. Frerichs,[1] B.A. Grierson,[4] R. A. Moyer,[5] C. Paz-Soldan,[2] D. Thomas,[2] E. A. Unterberg,[3] M. Wade[2]

[1]*University of Wisconsin-Madison, Madison, U.S.A.*
[2]*General Atomics, San Diego, U.S.A.*
[3]*Oak Ridge National Laboratory, Oak Ridge, U.S.A.*
[4]*Princeton Plasma Physics Laboratory, Princeton, U.S.A.*
[5]*University of California San Diego, La Jolla, U.S.A.*

E-mail: ehinson@wisc.edu

Abstract

Effective helium confinement time, $\tau_p{}^*{}_{,He}$, and its ratio with energy confinement, $\tau_p{}^*{}_{,He}/\tau_E$, are key metrics quantifying the suitability of fusion plasmas for a continuous burn. Comparisons in the DIII-D tokamak of discharges with suppression of edge localized modes (ELMs) by resonant magnetic field perturbations (RMPs) to the corresponding unperturbed ELMy discharges found that both of these metrics were strongly reduced, by a factor of approximately 2, after application of the RMPs. This reduction in $\tau_p{}^*{}_{,He}$ during RMP ELM suppression was observed in the plasma core, edge, and pumping plenum, where higher neutral helium concentration during RMPs was also measured. These findings provide evidence that future devices employing RMP ELM suppression may meet or even exceed the helium exhaust provided by the ELMs themselves, reducing helium ash, and thus maintaining high fusion gain.

Keywords: helium, resonant magnetic perturbations, edge-localized modes

1. Introduction

Future fusion devices, such as the ITER, based on the fusion of deuterium and tritium (D-T) must necessarily contend with helium as the "ash" byproduct. Continuous operation is not possible above a maximum level of helium content in the plasma, where excessive dilution of the D-T fuel and radiation of plasma thermal energy occurs [1]. This maximum level of helium at a fusion power gain of Q=5 is quantified by a limit to the ratio of the effective confinement time of helium, $\tau_{p^*,He}$, - the e-folding time for confined helium particles including recycling at the wall - to that of the plasma energy confinement time, τ_E: $\tau_{p^*,He}/\tau_E < 10$ [2]. Past experiments [3,4] have shown that H-mode, an operational regime characterized by favorable energy confinement [5,6] can be compatible with this limit. However, improved confinement during H-mode leads to gradients exceeding that permitted by magnetohydrodynamic (MHD) stability. Periodic MHD instabilities generated at the plasma edge, known as "Edge Localized Modes" or ELMs, provide for this particle exhaust. While H-mode plasmas have been observed to benefit from enhanced removal of non-hydrogenic contaminating nuclei during ELMs, or "ELM impurity flushing" [7], the heat loads imparted to plasma-facing components by the hot plasma expelled during these instabilities are expected to exceed engineering limits in large future devices.

In order to provide for necessary particle exhaust during H-mode confinement whilst avoiding the dangerous transient heat loading on plasma-facing surfaces characteristic of ELMs, a variety of ELM suppression and mitigation schemes are under investigation. One such scheme for ELM suppression is the application of 3-D perturbing magnetic fields, "resonant magnetic perturbations," (RMP) to the dominantly axisymmetric magnetic field [8]. A set of such coils is planned for ITER [9,10].

A critical issue arising for any ELM-suppression scheme is whether acceptable limits to helium contamination can still be maintained during suppression, [11] when the ELM impurity flushing process is removed. In this Letter, it is shown for the first time that H-mode plasmas using ELM suppression by RMP can be robust to helium contamination, and that the ELM flushing can be replaced by the RMP effect on helium transport. These results build on recent experimental work [12,13] establishing this additional use of RMP ELM suppression as a tool for impurity control.

The DIII-D tokamak is capable of reliable ELM suppression with applied RMP fields [14–17]. It is equipped with six window-framed coils (inside of the

 © xxxx IOP Publishing Ltd

confining toroidal field coils) in two rows, which were operated in "even parity" configuration for this work, where current polarity of the upper and lower row of coils is identical, alternating in the toroidal direction only. The cryopump used for plasma density control was frosted with a 1800 torr-L puff of Ar gas before each discharge in this work, which condenses to an approximately 2μm layer on the cryopump and substantially increases helium pumping [4,18]. Indeed, from [18], helium pumping speeds between 1.0×10^4 and 1.5×10^4 L/s are expected for the conditions in this work.

2. Experiment

A reduction of helium contamination during RMP ELM suppression is evident in a broad range of measurements in ELM-suppressed discharges versus unperturbed ELMy conditions. An approximate factor of 2 enhancement in He global exhaust, measured through a consistent reduction in $\tau_{p*,He}$, is observed in the ELM-suppressed state. Lower single null 'ITER-like' plasmas at ITER-relevant low electron pedestal collisionality ν_e*~0.3-0.4 are investigated, with toroidal field B_T = -1.96 T, plasma current I_p = 1.6MA, edge q_{95}=3.4-3.5, and RMP coil currents in the range 3.5-4.8 kA applied from 2000ms. For the discharges examined, helium was introduced at 3.0s and 4.0s, into stable plasma conditions, using identical 50ms helium gas puffs with an injection rate of 1.0×10^{21} particles/s in the upper outboard region. A third helium puff at 5.0s was also introduced but inconsistencies with neutral beam power after 5.0s significantly complicate this data. Two RMP cases are compared to the unperturbed H-mode (DIII-D discharge #169514): Case 1 (DIII-D discharge #169513), which had identical injected power as the H-mode case (6.45MW), and Case 2 (DIII-D discharge #169515), which had full ELM suppression, but at slightly lower power (5.6MW). The first helium puff of Case 1 had isolated ELMs, and for this reason is excluded from the comparative analysis of τ_p*,He.

In the following, data characterizing helium exhaust in four characteristic locations is reviewed. These locations include: the neutral particle reservoir (pumping plenum), the plasma core (rho~0.2), the plasma edge (pedestal region inside the separatrix in the good flux surface domain), and the plasma scrape-off layer (the 'SOL' or open field line domain). The effective helium confinement time τ_p*,He is obtained from exponential fits to the data. Finally, for each discharge, the mean value of τ_p*,He from these locations is compared to the energy confinement time, τ_E.

3. Helium Measurements

A Penning gauge with spectroscopic views was used to measure neutral helium and deuterium gas partial pressures in the pumping plenum, p_{He},, p_{D2}. The neutral pressures are a function of their constituent species' atomic neutral line emission intensities, and can be inferred by comparison to calibrations done in non-plasma conditions [14]. During RMP ELM suppression, substantially more helium was observed outside the confined plasma. Figure 1a shows the increase of helium concentration, $C_{He} = p_{He}/(p_{He}+p_{D2})$, at the pump during RMP application. Helium gas puffs at 3.0s and 4.0s are indicated in Fig 1a with the output of internal pressure sensors. These sensors are scaled to indicate the gas flow rate using calibrations obtained by comparison to pressure gauges in operations without plasma. The signals have been scaled to units of torr-L-s^{-1}/100, and were essentially identical between discharges. In subsequent figures they are indicated as shaded bars. Times of isolated ELMs occurring in the RMP discharge are indicated with vertical bars.

Fig. 1b shows the corresponding helium neutral partial pressures during these cases, with over-plotted exponential fits, taken between 3400-4000ms and 4400-5000ms.

Both the helium concentration and partial pressure are strongly increased in RMP cases compared to the ELMy cases. Because higher neutral pressure at the pump induces faster pumping, and all puffs were the same size, reduced τ_p*,He is already expected from particle conservation. The sustained higher *concentrations* of helium during RMP show that the increase in helium exhaust exceeded that occurring due to deuterium 'pumpout,' indicating a preferential impact on the helium. Decay times of the helium obtained from fits to partial pressure in Fig. 1b are graphed in Fig. 2. The value of τ_p*,He for RMP Case 1 was 1.2s, and for RMP Case 2 it was 1.6s and 1.4s for the first and second puff, respectively. Fits to the helium pressure for the ELMy discharge obtained τ_p*,He values of 6.2s and 5.4s for puffs 1 and 2, respectively.

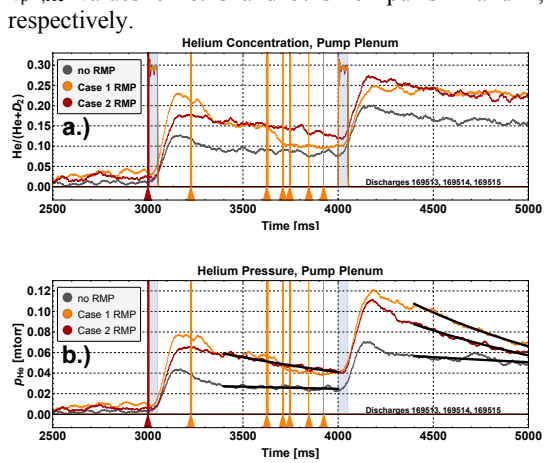

Fig. 1: Time evolutions of helium concentrations, a.) and pressures, b.), in the pumping plenum for Cases 1 and 2 vs the unperturbed H-mode. Fits to the data between 3400-4000ms and 4400-5000ms are plotted over the pressure data. ELMs are indicated with vertical bars, shaded according to the suppressed case in which they occurred. In a.), pressure sensor output from the gas valves for each of the 3

 © xxxx IOP Publishing Ltd

discharges is also plotted against the left axis in units of torr L s^{-1} /100.

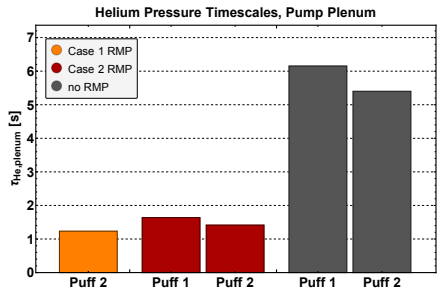

Fig. 2: Measured decay times of helium pressure in the pump plenum.

Helium levels measured in the core are consistent with the trends observed at the pump. Core ($\rho = 0.20$) helium plasma density n_{He} was measured using charge exchange recombination (CER) spectroscopy on the 304nm He-II emission line using the SPRED spectrometer at DIII-D. Figure 3 shows fits to the n_{He} time evolutions between 3250-4000ms, and 4250-5000ms. These measurements have been corrected for beam attenuation by the plasma [19].

The value of n_{He} for RMP cases is generally always less than for ELMy cases, but large uncertainties in the measurements due to ELM contamination in the ELMy case exist. While these are omitted in Figure 3a for clarity, when propagated to the resulting fits, values of $\boldsymbol{\tau}_p{}^*{}_{,He}$ appear highly uncertain. Nonetheless, all values of $\boldsymbol{\tau}_p{}^*{}_{,He}$ are shown in Figure 3b, and it can be seen that trends in $\boldsymbol{\tau}_p{}^*{}_{,He}$ between RMP/ELMy types, as well as between individual puffs within the ELMy case are maintained.

The specific values of $\boldsymbol{\tau}_p{}^*{}_{,He}$ were 1.6s for Case 1, 1.0s and 1.2s for puffs 1 and 2 of Case 2, respectively, and 4.7s and 4.3s for the ELMy case for puffs 1 and 2 respectively. Core electron densities n_e held roughly steady in the range of ~5x10^{19} m^{-3} for RMP cases and ~7x10^{19} m^{-3} for the noRMP cases.

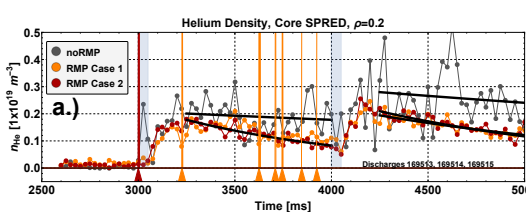

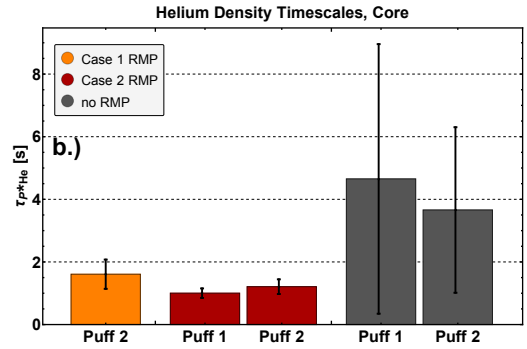

Figure 3: a.) Core CER measurements of helium density. b.) Associated time constants $\boldsymbol{\tau}_p{}^*{}_{,He}$ with standard error.

A representative measurement of n_{He} from the set of tangentially-viewing edge outer-midplane CER diagnostics ($\rho = 0.81$) is shown in Fig. 4a, and again a faster decay of helium in the RMP cases is observed. The mean of $\boldsymbol{\tau}_p{}^*{}_{,He}$ obtained from the data in Fig. 4a as well as two additional edge charge exchange chords located at $\rho = 0.86$ and $\rho = 0.91$, obtained from fits between 3250-4000 ms, and 4250-5000 ms are given in Fig. 4b. Values of $\boldsymbol{\tau}_p{}^*{}_{,He}$ are: 1.5s for Case 1, 1.6s and 1.7s for Case 2 for puffs 1 and 2, respectively, and 3.5s and 2.7s for the ELMy case for puffs 1 and 2, respectively. Pedestal n_e was steady, particularly for ELMy H-mode cases, though an increase of <20% of the edge n_e was visible in RMP cases just after each helium injection.

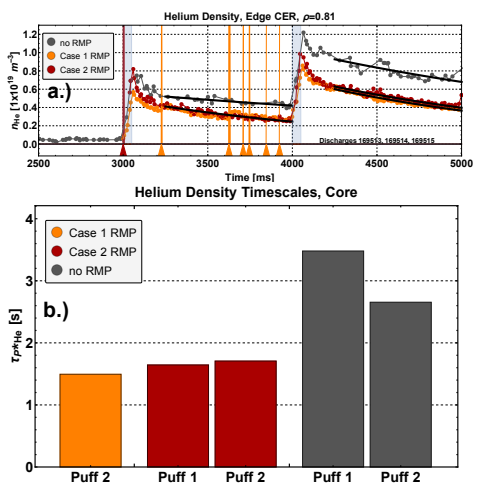

Fig. 4. a.) Edge midplane helium density from CER. ELMs are indicated with arrows on axis and vertical bars. Fits of the data between 3250-4000ms and 4250-5000ms are overplotted. b.) Decay times $\boldsymbol{\tau}_p{}^*{}_{,He}$ from fits to n_{He} in a.).

The reductions of helium in plasma regions, and corresponding increases in neutral inventories in the foregoing data show helium was better retained outside the confined plasma during RMPs. In other words, the fraction of all helium particles residing at the pump, as opposed to residing in plasma regions, was increased. This induces more efficient pumping

 © xxxx IOP Publishing Ltd

for a given amount of total helium, and a corresponding decrease in $\tau_p^*{}_{,He}$.

Measurements of helium proxies also add support to the picture of helium being retained outside the confined plasma regions during RMPs. Data from a spectrometer measuring 468.6 nm ionized helium line emission near the inner strike point (ISP) with background continuum subtraction is shown in Fig. 5. Much more helium photoemission was measured in the RMP cases. In comparison, D_α emission at the ISP, although quite dynamic for the ELMy discharge, was increased by less than a factor of 2 during RMPs.

Decay times for the helium photoemission were measured that roughly match those found for helium pressure and density – 1.1s for the Case 1, and 1.6s and 1.3s for puffs 1 and 2 in Case 2, respectively. Photoemission for the ELMy variant in these cases exhibited 3.8s and 3.4s decay times after an ELM subtraction procedure where a trimmed mean filter was used to remove ELM transients before fitting. Resulting decay times for the ELMy case depend on the details of this filter, but are found to be in any case generally >3.0s. These data also support the effective retention in the unconfined region observed in this experiment.

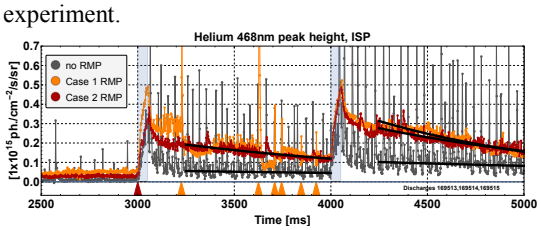

Fig. 5. Helium light from a spectrometer viewing the inner strike point. ELMs are marked below with arrows.

Values of $\tau_p^*{}_{,He}/\tau_E$, were obtained from the mean of $\tau_p^*{}_{,He}$ during relevant puffs (the second for Case 1, both for Case 2 and the ELMy case) using the Penning gauge, core and edge CER chords, and the mean value of τ_E over the same interval. The results are shown in Table 1. The overall reduction of $\tau_p^*{}_{,He}/\tau_E$ observed here was approximately a factor of two during RMP ELM suppression.

TABLE 1. $\tau_p^*{}_{,He}/\tau_E$ reduced during RMP

	Case 1	Case 2	noRMP
τ_E	0.13s	0.14s	0.19s
$<\tau_p^*{}_{,He}>$	1.4s	1.4s	4.3s
$\tau_p^*{}_{,He}/\tau_E$	11.	10.	23.

4. Discussion

It was shown for the first time in a diverted tokamak that $\tau_p^*{}_{,He}$ can be decreased by a factor of 2-3 during RMP ELM suppression. This result was shown for ITER relevant conditions - H-mode discharges in an ITER-similar shape, and at ITER relevant low pedestal electron collisionality.

The differences observed in helium neutral pressure at the pump already imply this result. Indeed, to more effectively exhaust helium, it would be sufficient if the He partial pressure were increased merely *in proportion* with D_2, since deuterium fuel can always be reintroduced as necessary in a functioning fusion device. However, the higher He concentration in RMP cases suggests that the effect is not a straightforward result of generic loss of confinement affecting the deuterium majority species, or particle 'pumpout,' but an effect preferentially impacting the helium. Whether this results from a dependence on atomic number Z of the 'pumpout' effect is among the questions raised by this work.

Fig. 6 shows normalized traces of helium measurements from Case 2, exemplifying the convergence to globally consistent values of $\tau_p^*{}_{,He}$ in all reservoirs. The transient timescales during and just after injection reflect the fast processes of transport between reservoirs and time-evolving global recycling, addressed in e.g. [4,20], before an equilibrium between reservoirs is established and the time evolution of the individual reservoirs is governed by net flows exhausted to the pump. This is the key timescale for long-term removal of helium, and fits for $\tau_p^*{}_{,He}$ have thus been applied to this region only. A manuscript addressing the faster-timescale behavior during and shortly after the injection is currently in preparation.

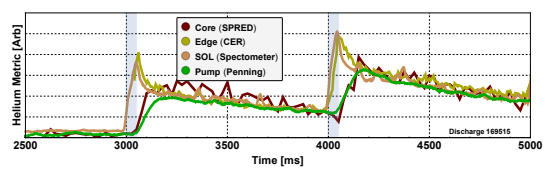

Fig. 6. Normalized traces of helium metrics for Case 2.

Many possible effects could contribute to the enhanced transport during RMP-ELM suppression observed here. Possible mechanisms include increased edge transport with increasing levels of stochasticity further outside the last closed flux surface, global changes to the plasma due to RMP altering neoclassical transport, and turbulence changes due to during RMP. Additionally, the changes RMPs induce in the SOL plasma can affect impurity force balance there, so as to increase helium exhaust. In particular, an increase in the friction force relative to the temperature gradient force as has been found in modeling of helium transport in the stellarator LHD during application of magnetic perturbations [21].

Increased impurity transport in the SOL during RMPs can also arise due to a simple mechanism classically envisioned for radial transport in the SOL [22]. In the original model, flux tubes with unfavorable force balance and long 1-D impurity confinement times can be depleted by outward radial cross-field transport, into less-collisional flux tubes, wherein impurities are more free to stream to divertor surfaces.

 © xxxx IOP Publishing Ltd

Thus, transport into the radial dimension 'short circuits' otherwise confining flux tubes, reducing the effective impurity trapping time to the timescale for radial transport. RMPs may be imagined to add a 3rd, poloidal, dimension into which diffusing impurities may escape. The high poloidal mode number perturbation of the lobes introduced by RMPs breaks up a formerly homogenous poloidal zone into heterogenous one, in which individual flux tubes with lower impurity trapping times can 'short circuit' their poloidal neighbors.

The findings reported here support enhanced He exhaust as an additional, critically important feature of the RMP ELM control scheme planned for use at ITER. Increased He retention was observed in the plasma periphery during RMP application, an essential precondition for enhanced removal by the pump. Corresponding reductions in helium effective particle confinement time, $\tau_{p^*,He}$, were also observed. While reduced $\tau_{p^*,He}$ during RMPs would be important on its own, regardless of its impact on τ_E, it is particularly promising that the initial results obtained here also include reductions in $\tau_{p^*,He}/\tau_E$, indicating stronger reductions in helium confinement versus that of energy. Thus the view that RMPs suppress ELMs and protect plasma-facing surfaces at the expense of a drop in energy confinement may well be excessively pessimistic, in that it disregards the fuller context, where D-T fusion's byproduct is considered. Accounting for an improvement in $\tau_{p^*,He}/\tau_E$ such as that shown here could in fact render those plasmas more promising candidates for realizing fusion.

Acknowledgements

This work is supported by the U.S. Department of Energy, Office of Science, Office of Fusion Energy Sciences, using the DIII-D National Fusion Facility, a DOE Office of Science user facility, under Awards DE-FC02-04ER54698. Work also supported by US DOE Early Career Award DE-SC0013911, DE-AC05-06OR23100, DE-FG02-07ER54917, DE-AC05-00OR22725, and DE-AC04-94AL85000. DIII-D data shown in this paper can be obtained in digital format by following the links at https://fusion.gat.com/global/D3D_DMP.

Disclaimer: This report was prepared as an account of work sponsored by an agency of the United States Government. Neither the United States Government nor any agency thereof, nor any of their employees, makes any warranty, express or implied, or assumes any legal liability or responsibility for the accuracy, completeness, or usefulness of any information, apparatus, product, or process disclosed, or represents that its use would not infringe privately owned rights. Reference herein to any specific commercial product, process, or service by trade name, trademark, manufacturer, or otherwise does not necessarily constitute or imply its endorsement, recommendation, or favoring by the United States Government or any agency thereof. The views and opinions of authors expressed herein do not necessarily state or reflect those of the United States Government or any agency thereof.

References

[1] Loarte A, et al, 2007 Chapter 4: Power and particle control *Nucl. Fusion* **47** S203–63

[2] Reiter D, Wolf G H and Kever H 1990 Burn condition, helium particle confinement and exhaust efficiency *Nucl. Fusion* **30** 2141–55

[3] Wade M R, Hillis D L, et al, 1995 Helium transport and exhaust studies in enhanced confinement regimes in DIII-D *Phys. Plasmas* **2** 2357–65

[4] Wade M R, Hillis et al, Mioduszewski P K and DIII-D Team D-D 1995 Helium Exhaust Studies in H -Mode Discharges in the DIII-D Tokamak Using an Argon-Frosted Divertor Cryopump *Phys. Rev. Lett.* **74** 2702–5

[5] Wagner F, et al, 1982 Regime of Improved Confinement and High Beta in Neutral-Beam-Heated Divertor Discharges of the ASDEX Tokamak *Phys. Rev. Lett.* **49** 1408–12

[6] Wagner F, et al, 1984 Development of an Edge Transport Barrier at the H-Mode Transition of ASDEX *Phys. Rev. Lett.* **53** 1453–6

[7] Groebner R J 1993 An emerging understanding of H-mode discharges in tokamaks * *Phys. Fluids B Plasma Phys.* **5** 2343–54

[8] Evans T E, et al 2004 Suppression of large edge-localized modes in high-confinement DIII-D plasmas with a stochastic magnetic boundary *Phys. Rev. Lett.* **92**

[9] Martin A, et al, 2013 Design evolution and integration of the ITER in-vessel components *Fusion Eng. Des.* **88** 1955–9

[10] Evans T E, Orlov D M, Wingen A, Wu W, Loarte A, Casper T A, Schmitz O, Saibene G, Schaffer M J and Daly E 2013 3D vacuum magnetic field modelling of the ITER ELM control coil during standard operating scenarios *Nucl. Fusion* **53** 093029

[11] Grierson B A, et al, 2015 Impurity confinement and transport in high confinement regimes without edge localized modes on DIII-Da) *Phys. Plasmas* **22** 055901

[12] Schmitz O, et al 2016 Enhancement of helium exhaust by resonant magnetic perturbation fields at LHD and TEXTOR *Nucl. Fusion* **56** 106011

[13] Unterberg E A, Schmitz O, Evans T E, Maingi R, Brooks N H, Fenstermacher M E, Mordijck S, Moyer R A and Orlov D M 2010 The effects of an open and closed divertor on particle exhaust during edge-localized mode suppression by resonant magnetic perturbations in DIII-D *Nucl. Fusion* **50** 034011

[14] Evans T E, et al, 2008 RMP ELM suppression in DIII-D plasmas with ITER similar shapes and collisionalities *Nucl. Fusion* **48** 024002

[15] Schmitz O, Evans T E, Fenstermacher M E, Lanctot M J, Lasnier C L, Mordijck S, Moyer R A and Reimerdes H 2014 Formation of a three-dimensional plasma boundary after decay of the

 © xxxx IOP Publishing Ltd

plasma response to resonant magnetic perturbation fields *Nucl. Fusion* **54** 012001

[16] Paz-Soldan C, Nazikian R, Haskey S R, Logan N C, Strait E J, Ferraro N M, Hanson J M, King J D, Lanctot M J, Moyer R A, Okabayashi M, Park J-K, Shafer M W and Tobias B J 2015 Observation of a Multimode Plasma Response and its Relationship to Density Pumpout and Edge-Localized Mode Suppression *Phys. Rev. Lett.* **114** 105001

[17] Nazikian R, et al 2015 Pedestal Bifurcation and Resonant Field Penetration at the Threshold of Edge-Localized Mode Suppression in the DIII-D Tokamak *Phys. Rev. Lett.* **114** 105002

[18] Menon M M, Laughon G J, Maingi R, Wade M R, Hillis D L and Mahdavi M A 1995 Pumping characteristics of a cryopump with Ar sorbent in He and in a D_2 /He mixture *J. Vac. Sci. Technol. A Vacuum, Surfaces, Film.* **13** 551–5

[19] Grierson B A, Burrell K H, Chrystal C and Haskey S R 2018 Relative intensity calibration of the DIII-D charge-exchange recombination spectroscopy system using neutral beam injection into gas *Rev. Sci. Instrum.* **89** 10D116

[20] Roth J, Krieger K and Fussmann G 1992 Divertor retention for recycling impurities *Nucl. Fusion* **32** 1835–44

[21] Bader A, Kobayashi M, Schmitz O, Akerson A R, Effenberg F, Frerichs H, Feng Y, Hegna C C, Ida K and Group T L E 2016 Modeling of helium transport and exhaust in the LHD edge *Plasma Phys. Control. Fusion* **58** 124006

[22] Stangeby P . and Elder J . 1995 Impurity retention by divertors. I. One dimensional models *Nucl. Fusion* **35** 1391–412

 © xxxx IOP Publishing Ltd